Exploiting Non-Reciprocity in BOTDA systems

A. Lopez-Gil,[1] X. Angulo-Vinuesa,[1] A. Dominguez-Lopez,[1] S. Martin-Lopez,[1] and M. Gonzalez-Herraez[1]

[1] *Departamento de Electrónica, Universidad de Alcalá, Edificio Politécnico, 28805 Alcalá de Henares, Madrid (Spain)*
**Corresponding author: alexia.lopez@uah.es*

Received Month X, XXXX; revised Month X, XXXX; accepted Month X, XXXX; posted Month X, XXXX (Doc. ID XXXXX); published Month X, XXXX

In this paper, we present and demonstrate a novel technique for distributed measurements in Brillouin Optical Time-Domain Analysis (BOTDA) based on the use of the nonlinear phase-shift induced by stimulated Brillouin scattering (SBS). Employing a Sagnac Interferometer (SI), the position-resolved Brillouin Phase-shift Spectrum (BPS) along the fiber can be obtained, benefiting from the sensitivity to non-reciprocal phase-shifts of the SI scheme. This proposal simplifies the existing methods to retrieve the BPS distribution along an optical fiber since no phase modulation, no filtering and no high-bandwidth detectors are required. The fundamentals of the technique are described theoretically and validated through numerical simulations and experimental measurements.

OCIS Codes: (060.2370) Fiber optics sensor; (290.5900) Scattering, stimulated Brillouin; (999.999) Brillouin optical time domain analysis; (999.999) Brillouin distributed sensors; (190.0190) Nonlinear optics.

In recent years, Brillouin-based distributed temperature and strain fiber sensors have become strong competitors of conventional multipoint sensing systems thanks to their unique properties, among them, their ability to sense hundreds or thousands of points over a single optical fiber. Brillouin Optical Time Domain Analysis (BOTDA) systems [1], one of the most common techniques, has evolved into a consolidated fiber sensing technology that is widely used for temperature and strain monitoring over an extended distance range (several tens of kilometers) with meter-scale spatial resolution. Also, shorter distances can be monitored with sub-meter spatial resolutions.

The underlying physical phenomenon of a BOTDA is the optical effect denominated Stimulated Brillouin Scattering (SBS) [2]. This effect is an acousto-optic process that couples light between two counter-propagating waves by means of an induced acoustic wave. The SBS is a nonreciprocal process since the photons are scattered only in one direction owing to the generated acoustic wave nature. In practical terms, SBS manifests as a counter-propagating narrowband amplification curve (in a spectral region around $\nu_0 - \nu_B$) and an attenuation one (in a spectral region around $\nu_0 + \nu_B$) when an intense and coherent pump light beam (ν_0) is fed into one of the ends of the optical fiber. The Brillouin Gain Spectrum (BGS), shows a Lorentzian gain distribution and a Brillouin phase profile, called Brillouin Phase-shift Spectrum (BPS).

Conventionally, BOTDA systems measure the Gain and Loss mechanisms of SBS, because they are straightforward to retrieve with direct detection. To provide the distributed characteristic to the BOTDA, the pump wave is pulsed and an amplified/attenuated probe signal is analyzed as a function of the time-of-flight of the pump pulse in the fiber. By fitting the gain/loss profile in every point, one is able to determine the Brillouin Frequency Shift (BFS, ν_B), from which the variations of temperature or strain can be extracted [3].

Some previous works have also paid attention to measuring the distributed BPS [4-7]. All these systems employ complex phase modulation setups to obtain the probe signal and usually require very high–bandwidth photo-detectors and digitizing elements. Recently, another proposal has been developed utilizing acousto-optic phase shifting and IQ demodulation [8]. This allows avoiding the phase modulation but increases the measuring time. Interestingly, the BPS has a linear shape near the BFS, which changes also with the strain/temperature changes. This feature can be used to perform dynamic measurements [5]. Moreover, this sensing scheme has been demonstrated to be immune to non-local effects (depletion) [4].

In this paper, we propose and demonstrate a novel BOTDA technique that exploits the non-reciprocity of SBS to make simplified and fully distributed measurements of BPS along an optical fiber. The core of the proposal lies in using a Sagnac Interferometer (SI) [9-10] within a conventional BOTDA setup. The SI provides sensitivity to SBS thanks to the non-reciprocal nature of this acousto-optic interaction. The proposal simplifies the already existing BPS measurement methods since no phase modulation or high-bandwidth detector is necessary.

As mentioned above, a SI is added to the traditional BOTDA experimental setup. SI is a widely utilized interferometer to sense nonreciprocal effects thanks to its environmental robustness [9-10]. The SI is formed by a 50/50 polarization-independent fiber-optic coupler, the Fiber Under Test (FUT), and a polarization controller (PC). Fig. 1 shows the schematic representation of the introduced SI, and the routes followed by pump and probe signals. As it is visible, a dual-sideband (DSB) modulated probe is introduced into the FUT through the input coupler. The coupler splits the probe beam in two counter-propagating beams, which travel along the FUT in opposite directions (labeled PROBE 1 and PROBE 2 in the Fig.1) and recombine again at the coupler. Conventionally, the PC is set to have perfect alignment in the output polarization states upon recombination. This, in principle, ensures that the two beams have followed reciprocal paths. If this is the case, the transmitted field is zero while the

reflected field is maximum, and the setup behaves as a mirror for the probe beam (in this case a lossy mirror).

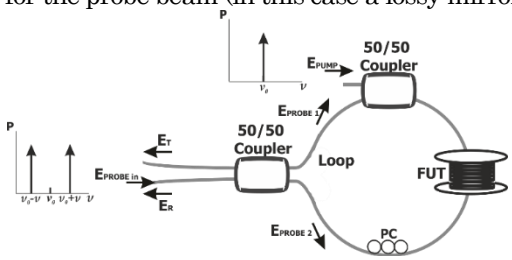

Fig. 1. Schematic representation of a Sagnac Interferometer (SI). E_T: Transmitted electric field; E_R: Reflected electric field; PC: Polarization Controller; FUT: Fiber Under Test. ν_0: pump frequency.

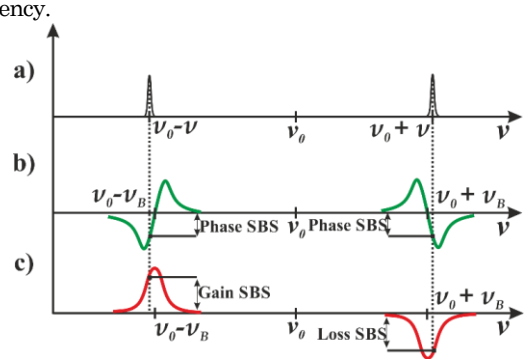

Fig. 2. SBS interaction experienced by the two sidebands of PROBE 2 after travelling along the SI. (a) Probe spectrum (b) Brillouin phase-shift profile for both sidebands, showing that the two sidebands experience the same phase shift and (c) gain and loss curves showing that both sidebands suffer complementary amplitude responses. ν_0: pump frequency.

Unlike the conventional SI case, in which the PC is adjusted to have perfect polarization alignment at the output, here the polarization controller is adjusted to ensure a certain polarization mismatch at the output. In absence of any pump wave, the transmitted and reflected fields are obtained from the partial interference between the counter-propagating probe waves. This condition automatically guarantees that there is a certain phase mismatch among the interfering waves [11] and, thus, the transmitted field is not zero. Also, in this case, the reflected field is not maximized. In our setup, we adjust the PC to have similar output powers in the transmitted and reflected output ports. This polarization mismatch acts as a certain "bias" for the interferometer.

The pulsed pump wave is introduced in the FUT using another 50/50 coupler within the fiber loop. This ensures that it interacts with only one of the probe waves (PROBE 2 in Fig.1), PROBE 1 acting only as a reference signal. Thus, the lower frequency sideband of PROBE 2 will be amplified and the higher frequency sideband of PROBE 2 will be attenuated exactly the same amount (for small gain values). The net power change of PROBE 2 will therefore be zero (to first order). However, simultaneously, both sidebands of PROBE 2 will suffer *the same nonlinear phase shift* (see Figure 2). The output of the SI will then be directly dependent on the shape of the phase shift and not on the gain or attenuation, as we will see below. This is critical in the behavior of the setup and will allow an extremely simple measurement method of the phase map as we will see later, with no filters required.

In order to illustrate the behavior of the proposed system, we provide a simple, scalar mathematical model of its operation. It essentially assumes that the interfering part of the counter-propagating beams shows a relative phase delay of 2ϕ. We have to analyze in each case the output signal obtained for the upper and lower frequency sidebands of the probe, both in transmission and in reflection. The interfering part of the transmitted light intensity for the lower frequency band can be written as:

$$|E_T|^2_{\nu_0-\nu} \propto |e^{-j\phi} - Ge^{+j\phi}|^2 \qquad (1)$$

while the upper frequency band has the following form:

$$|E_T|^2_{\nu_0+\nu} \propto |e^{-j\phi} - Ae^{+j\phi}|^2 \qquad (2)$$

Where ν_0 is the frequency of the pump wave employed.

The reflected light intensity equations for both frequency bands are similar to the transmitted ones but changing the – sign for a + sign (the phase difference between the two outputs of a coupler is $\pi/2$). In the above expressions, G (Brillouin gain) and A (Brillouin loss) are considered small enough to be linearized and approximated by:

$$G = e^{(g_B \cdot P_P \cdot \Delta z)} \approx 1 + g_B(\nu) \cdot P_P \cdot \Delta z \qquad (3)$$

$$A = e^{(-g_B P_P \cdot \Delta z)} \approx 1 - g_B(\nu) \cdot P_P \cdot \Delta z \qquad (4)$$

where P_p is the peak pump power and Δz is the pump pulse width. $g_B(\nu)$ is the complex Brillouin gain coefficient, defined as:

$$g_B(\nu) = g(\nu) + j\sigma(\nu) = \frac{g_P/A_{eff}}{1 + j\left(\frac{\nu - \nu_B}{\Delta\nu_B}\right)} \qquad (5)$$

where g_p is the Brillouin gain factor ($5 \cdot 10^{-11}$ m/W), A_{eff} is the effective area, ν is the optical frequency shift, ν_B is the BFS and $\Delta\nu_B$ is the Brillouin gain bandwidth.

It is now straightforward to recover meaningful expressions for the transmitted and reflected probe signals, and in analytic form. The AC part of the transmitted power ($|E_T|^2 = |E_T|^2_{\nu_0-\nu} + |E_T|^2_{\nu_0+\nu}$) results to be:

$$|E_T|^2 \propto 16\,\sigma(\nu)\sin(2\phi) - 8\sigma(\nu)\sin(4\phi) \qquad (6)$$

and the AC part of the reflected power ($|E_R|^2 = |E_R|^2_{\nu_0-\nu} + |E_R|^2_{\nu_0+\nu}$) can be written as:

$$|E_R|^2 \propto -16\,\sigma(\nu)\sin(2\phi) - 8\sigma(\nu)\sin(4\phi) \qquad (7)$$

As it is visible, as long as there is a phase delay between the two propagation directions $\phi \neq 0$, a signal proportional to the SBS phase shift can be extracted from either the transmitted or reflected light channels. Note that the recovered phase profile depends on the value of ϕ. Thus, the phase profile can be recovered inverted or non-inverted depending on the specific settings of the PC.

It is interesting to think what happens when we subtract the reflected light intensity to the transmitted light intensity. The result is easily computed to be:

$$|E_T|^2 - |E_R|^2 \propto 32\sigma(\nu)\sin(2\phi) \qquad (8)$$

Thus, it is simple to see that the amplitude of the phase response recorded in that case is doubled in comparison

with the single detector case. This situation would correspond to the use of a balanced detector among the transmission and reflection ports, as we will see in our experimental setup. In addition to doubling the amplitude of the signal, the balanced detection system makes the setup more robust to common-mode intensity noise [12].

To verify the above analysis, we have developed an experimental setup. The developed experimental setup is essentially a conventional BOTDA setup that has been modified to place the FUT in a Sagnac loop. The signals are introduced into the SI following the scheme in Fig.1 A schematic diagram of the whole experimental setup used for the tests is depicted in Fig. 3. It is based on a previously developed BOTDA setup [12] although, as aforementioned, it incorporates a simple set of optical elements to create the SI. As in most BOTDA schemes, in this setup both pump and probe waves are obtained from a single Distributed Feedback (DFB) laser diode [3]. The laser has a linewidth of 1.6 MHz. A Mach-Zehnder Electro-Optic Modulator (EOM) is used to obtain the dual-sideband (DSB) probe signal with suppressed carrier. The output probe power is controlled using a Variable Optical Attenuator (VOA), before being fed into the SI. The probe power fed at the input of the SI is in the order of ~1 mW on each sideband. The modulating frequency of the EOM is chosen to sweep around the BFS of the FUT (~10.88 GHz).

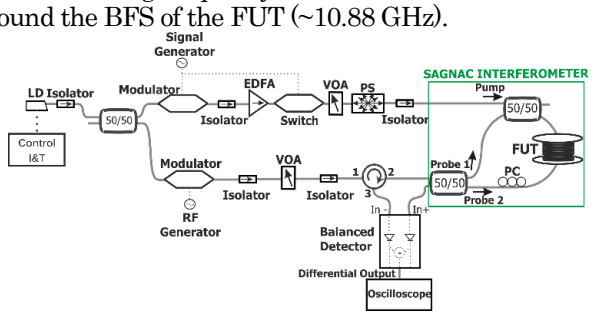

Fig. 3. Experimental setup of the BOTDA with balanced detection using a Sagnac Interferometer (SI). LD: Laser Diode; EDFA: Erbium Doped Fiber Amplifier; VOA: Variable Optical Attenuator; PS: Polarization Scrambler; RF: Radio-Frequency; PC: Polarization Controller; FUT: Fiber Under Test.

At the pump side, the signal is pulsed using another EOM. A high-speed switch is inserted in the scheme to improve the extinction ratio of the pulses obtained at the output of the EOM (~40 dB). After pulsing, the optical signal is amplified using an Erbium Doper Fiber Amplifier (EDFA) and the output power is also controlled using a VOA. The pulse peak power provided to the SI is ~60 mW. The polarization state of the pulse is scrambled to mitigate the polarization sensitivity of the interaction. The pump pulses are introduced into the fiber using another 50/50 coupler in the ring, as mentioned.

The input probe is split into PROBE 1 and PROBE 2 (by a 50/50 coupler) and introduced in opposite directions in the FUT. The lower frequency sideband of PROBE 2 will be amplified while the higher frequency one will be attenuated by SBS within the FUT as they interact with the introduced pump wave. Upon arrival at the coupler, PROBE 1 and PROBE 2 are recombined again and interfere as mentioned before. Note that the PC is adjusted to have approximately equal powers in the transmitted and reflected ports. This ensures a certain non-reciprocal phase shift between the two paths (clockwise and counter-clockwise). After recombination, the transmitted and reflected fields (E_T and E_R respectively) are introduced into the positive and negative ports of a balanced detection system. The differential output will be the outcome of subtracting the negative input signal (reflected light intensity) to the positive input signal (transmitted light intensity). The AC part of this signal provides the desired BPS profile, as stated previously.

As it happens with the BFS, the BPS always maintains the shape but its position in frequency with respect to the pump varies in response to changing strain or temperature conditions. In this technique, it is possible work with the center frequency of the slope of the phase-shift which equals to the BFS of the FUT (~10.88 GHz). In case of a temperature or strain event, the phase curve will locally be displaced proportionally to the suffered event.

Now we illustrate the results obtained with the BOTDA using the Sagnac configuration described previously. To accomplish these BOTDA measurements, a frequency sweep is done from 10.75 GHz to 11 GHz. The measurements have been performed using a Brillouin pump pulse-width of 25 ns (2.5 meter spatial resolution) over ~ 4.3 km of single-mode fiber (composed of two different fiber spools of 4 km and 300 m). The fiber has an effective area of 70 μm^2 and an essentially homogeneous BFS located at approximately 10.88 GHz at the pump wavelength (~1550 nm). To achieve a clean trace, the traces are averaged 1024 times.

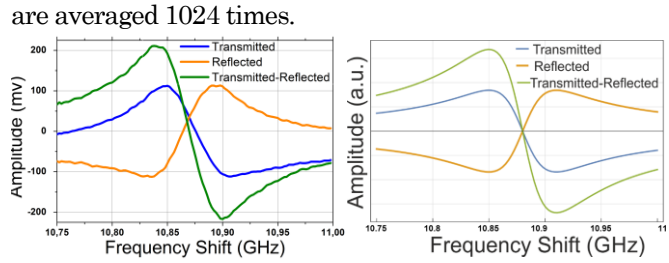

(a) (b)

Fig. 4. (a) Experimental transmitted light intensity (blue) and reflected light intensity (orange) together with the Brillouin Phase-Shift profile recovered in the balanced detector (green). The measurements have been done for a frequency sweep between 10.75 GHz and 11 GHz of the fiber under test. (b) Simulated results of this configuration.

In Fig 4(a). we can see the detected AC signal in transmission and reflection from the SI at a given spatial location (a given point of the fiber). As it can be observed, the transmitted and reflected intensities follow the phase profile of the SBS interaction, as predicted in Equations (6) and (7), while the balanced channel shows the phase contribution with double sensitivity, as expected. This figure is also consistent with the simulation results obtained using the model described above (Fig. 4(b)).

It is interesting now to go more into detail and check the actual behavior of the individual transmitted signals for both sidebands (gain and loss). Fig. 5(a) shows the signals corresponding to the gain and loss bands which have been individually measured (blue and orange curves) by using a narrowband-filtering scheme comprising a suitably tuned Bragg grating for a given location. As it is visible, the gain

band follows a distorted gain shape (the distortion corresponding to the phase contribution) and, similarly, the attenuation band follows a distorted loss shape. The sum of the two corresponds to the aggregate light transmission (green curve), which is roughly equivalent to the measured trace (blue curve in Fig.4a). Again, these measurements show good agreement with the expected behavior from the model, plotted in Fig. 5(b).

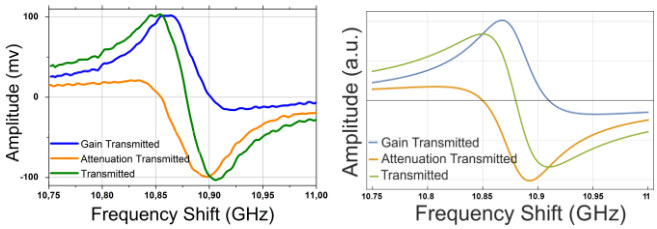

(a) (b)

Fig. 5. (a) Experimental transmitted light intensity in the lower frequency sideband (blue) and higher frequency sideband (orange) together with the overall transmitted light intensity (green). The measurements have been done for a frequency sweep between 10.75 GHz and 11 GHz of the fiber under test. (b) Simulated output from the analytical model for the same frequency sweep.

In Fig. 6 we depict the measurements of the phase-shift for the complete fiber length. Such outcome confirms the possibility of using this scheme to perform distributed BPS measurements. The phase profile at the midpoint of the FUT length presents residual pump power, which is mostly removed using the balanced detector.

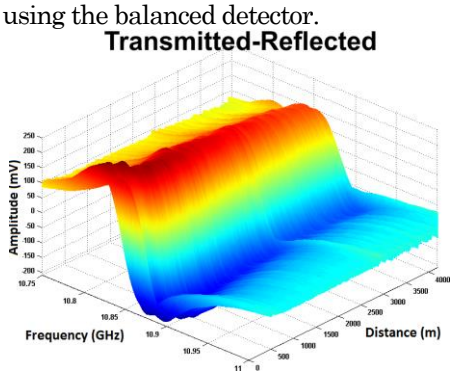

Fig. 6. BPS sweep for the complete fiber length. The probe signal frequency is swept from 10.75 GHz until 11 GHz and the traces are acquired with 25 ns pulses. Number of averages is 1024.

The performance of the setup as a sensor was verified by locating a hot spot at the end of the optical fiber (km. 4.3). This was done by introducing ~2.5 meters in a temperature-controlled oven at 85ºC. Fig. 7 shows the results of the BPS change in the hot-spot position (orange) in comparison with the same location in a room with a temperature of 25 ºC (blue). The frequency difference between these two profiles is approximately 80 MHz. Considering a sensitivity of 1.33 MHz/ºC in the Brillouin shift, this gives us a temperature variation of ~60 ºC, which is a good agreement with the expected temperature difference.

In conclusion, we have presented a technique to measure the distributed BPS profile along an optical fiber using a SI in combination with a BOTDA. This novel method reduces the complexity of the existing techniques to retrieve the BPS since no phase modulation and no high-bandwidth detectors are needed. Moreover, no optical filtering is needed either. The technique has been theoretically studied and proof-of-concept experiments have been performed to demonstrate its suitability.

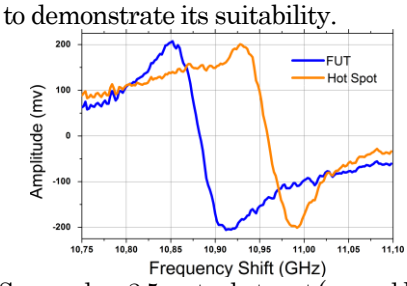

Fig. 7. BPS around a ~2.5-meter hot-spot (around km 4.3).

Acknowledgements

This work was supported in part by the European Research Council through U-FINE under Grant 307441, in part by the Spanish Ministry of Science and Innovation under Projects TEC2012-37958-C02-01, TEC2012-37958-C02-02 and TEC2013-45265-R, the INTERREG SUDOE program ECOAL-MGT, and in part by the Comunidad de Madrid under projects EDISON (CCG2014/EXP-072) and SINFOTON-CM:S2013/MIT-2790. The work of S. Martín-Lopez was supported by the Spanish Ministry of Science and Innovation through a "Ramón y Cajal" Contract.

References

1. T. Horiguchi and M. Tateda, J. Lightwave Technol., **7**, 1170 (1989)
2. G.P. Agrawal, Nonlinear Fiber Optics, 4th ed., San Diego, CA: Academic, 2007, ch. 9
3. M. Niklès, L. Thévenaz, and P. A. Robert, J. Lightwave Technol., **15**, 1842 (1997)
4. J. Urricelqui, M. Sagües, and A. Loayssa, Opt. Express, **21**, 17186 (2013)
5. J. Urricelqui, A. Zornoza, M. Sagües, and A. Loayssa, Opt. Express, **20**, 26942 (2012)
6. M. Dossou, D. Bacquet, and P. Szriftgiser, Opt. Letters, **35**, 3850 (2010)
7. X. Lu, M. A. Soto, M. Gonzalez-Herraez, and L. Thevenaz, in Proc. SPIE, **8794,** 87943P-1 (2013)
8. X. Tu, Q. Sun, W. Chen, M. Chen, and Z. Meng, IEEE Photonic. J., **6**, 6800908 (2014)
9. B. H. Lee, Y. H. Kim, K. S. Park, J. B. Eom, M. J. Kim, B. S. Rho and H. Y. Choi, Sensors, **12,** 2467 (2012)
10. B. Culshaw, Meas. Sci. Technol., **17**, R1 (2006)
11. L. Thévenaz, M. Niklès, and P. Robert, Proc. Symposium on Optical Fiber Measurements, **839**, 151 (1992)
12. A. Dominguez-Lopez, A. Lopez-Gil, S. Martin-Lopez and M. Gonzalez-Herraez, IEEE Photonic. Tech, **26**, 338 (2014)

Full Citation Listings

1. T. Horiguchi and M. Tateda, "BOTDA-nondestructive measurement of single-mode optical fiber attenuation characteristics using Brillouin interaction: theory" J. Lightwave Technol., **7**, 1170-1176 (1989).
2. G.P. Agrawal, *Nonlinear Fiber Optics*, 4th ed., San Diego, (Academic, 2007), ch. 9.
3. M. Niklès, L. Thévenaz, and P. A. Robert, "Brillouin gain spectrum characterization in single-mode optical fibers", J. Lightwave Technol., **15** (10), 1842-1851 (1997).
4. J. Urricelqui, M. Sagües, and A. Loayssa, "BOTDA measurements tolerant to non-local effects by using a phase-modulated probe wave and RF demodulation", Opt. Express, **21** (14), 17186-17194 (2013).
5. J. Urricelqui, A. Zornoza, M. Sagües, and A. Loayssa, "Dynamic BOTDA measurements based on Brillouin phase-shift and RF demodulation", Opt. Express, **20** (24), 26942-26949 (2012).
6. M. Dossou, D. Bacquet, and P. Szriftgiser, "Vector Brillouin optical time-domain analyzer for high-order acoustic modes", Opt. Letters, **35** (22), 3850-3852 (2010).
7. X. Lu, M. A. Soto, M. Gonzalez-Herraez, and L. Thevenaz, "Brillouin distributed fibre sensing using phase modulated probe", in Proc. SPIE, **8794,** 87943P-1 – 87943P-4 (2013).
8. X. Tu, Q. Sun, W. Chen, M. Chen, and Z. Meng, "Vector Brillouin Optical Time-Domain Analysis with Heterodyne Detection and IQ Demodulation Algorithm", IEEE Photonic. J., **6** (2), 6800908 (2014).
9. B. H. Lee, Y. H. Kim, K. S. Park, J. B. Eom, M. J. Kim, B. S. Rho and H. Y. Choi, "Interferometric Fiber Optic Sensors", Sensors, **12,** 2467-2486 (2012).
10. B. Culshaw, "The optical fibre Sagnac interferometer: an overview of its principles and applications", Meas. Sci. Technol., **17**, R1-R16 (2006).
11. L. Thévenaz, M. Niklès, and P. Robert, "Interferometric Loop Method for polarization Dispersion Measurements", Proc. Symposium on Optical Fiber Measurements, **839**, 151-154 (1992).
12. A. Dominguez-Lopez, A. Lopez-Gil, S. Martin-Lopez and M. Gonzalez-Herráez, "Signal-to-Noise Ratio Improvement in BOTDA Using Balanced Detection", IEEE Photonic. Tech, **26** (4), 338-341 (2014).